AD-A060 108 ADMIRALTY UNDERWATER WEAPONS ESTABLISHMENT PORTLAND --ETC F/G 20/1
DIFFRACTION AROUND FINITE PLANAR BAFFLES.(U)
JUN 78 D T WILTON

UNCLASSIFIED AUWE-ACC-46291 DRIC-BR-64757 NL

1 OF 1
AD
A060108

END
DATE
FILMED
12-78
DDC

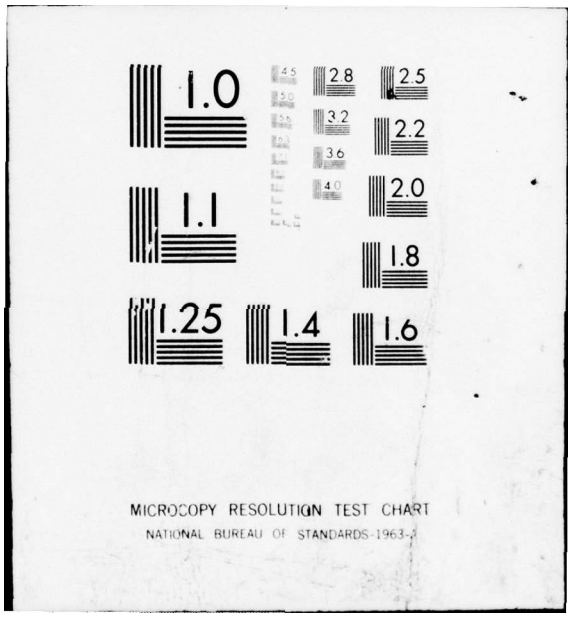
1.0
1.1
1.25
1.4
1.6
1.8
2.0
2.2
2.5
2.8
3.2
3.6
4.0
4.5
5.0
5.6
MICROCOPY RESOLUTION TEST CHART
NATIONAL BUREAU OF STANDARDS-1963-A

U.D.C. No. 623.983:
532.559.8:
534.26

Divisional Note No 46291
Date: (11) June 1978
Copy No: 39

(18) DRIC

(19) BR-64757

(1) Divisional note,

(6)

DIFFRACTION AROUND FINITE PLANAR BAFFLES

by

(10) D. T./Wilton

(12) 30pp

(14) AUWE-ACC-46291

ADMIRALTY UNDERWATER WEAPONS ESTABLISHMENT,
PORTLAND

Div Note No. 46291

Divisional Notes provide a permanent record of the results of those investigations carried out in the Establishment which are not considered suitable for issue as Establishment Reports or Technical Notes. They are not normally circulated outside the Establishment and extracts are not to be quoted in any official correspondence.

CONTENTS

ILLUSTRATIONS

Figure

ILLUSTRATIONS (Cont'd)

Divisional Note No. 46291
June 1978

DIFFRACTION AROUND FINITE PLANAR BAFFLES

PRÉCIS

1. The diffraction of sound around the edge of a half plane is considered in order to gain some insight into the effect of positioning sonar arrays on or near finite baffles. Some useful approximations are derived and demonstrated for the pressure levels due to a single source at endfire and also directly behind both soft and hard baffles. Comparisons are made with the assumption of an infinite baffle and the usual approximation for dealing with an array on a finite hard baffle is questioned.

INTRODUCTION

2. This note considers the diffraction of sound around the edge of a half plane in order to gain some insight into the effect of positioning sonar hydrophones and arrays on or near finite baffles.

3. It is of particular interest to determine the influence of a finite baffle upon the diffracted field at endfire, and also the effect of different baffle impedances upon the field behind the baffle.

4. Normally when considering the directivity pattern of an array in the presence of a finite baffle, a multiplicative factor is suggested as a modification to the relatively easily computed infinite baffle pattern. The necessity and correctness of this procedure for soft and hard baffles is also discussed.

THEORY

5. The theoretical model is based upon the results of a previous note concerned with diffraction in the presence of a wedge-shaped baffle (Reference 1).

6. The normalised farfield pressure of a point source located at (ρ_o, ϕ_o, z_o) in the presence of an acoustically soft wedge enclosing an angle α is given by

$$P(\theta,\phi) = \frac{2\pi}{\alpha} e^{ikz_o\cos\theta} \sum_{n=o}^{\infty} \epsilon_n \sin\frac{n\phi\pi}{\alpha} \sin\frac{n\phi_o\pi}{\alpha} i^{n\pi/\alpha} J_{n\pi/\alpha}(k\rho_o \sin\theta) \qquad (1)$$

($\epsilon_o = 1$, $\epsilon_n = 2$ for $n = 1,2,\ldots$). The geometry for this problem is shown in Figure 1. The farfield pressure has been normalised with respect to the free-field pressure of the source of strength P_o at the farfield distance R ($= P_o e^{-ikR}/4\pi R$). A harmonic time dependence $e^{i\omega t}$ is assumed throughout and omitted and k ($= \omega/c = 2\pi/\lambda$) is the wavenumber, where c is the speed of sound in the fluid and λ is the wavelength at angular frequency ω.

7. A half plane is the special case of a wedge when the wedge angle α is allowed to be 2π radians. The baffle is thus infinitely thin and perfectly reflecting such that there is no transmission through the baffle. In this case expression (1) reduces to

$$P(\theta,\phi) = e^{ikz_o\cos\theta} \sum_{n=o}^{\infty} \epsilon_n \sin\frac{n\phi}{2} \sin\frac{n\phi_o}{2} e^{in\pi/4} J_{n/2}(k\rho_o \sin\theta) \qquad (2)$$

8. A more convenient representation both to obtain limiting values and for numerical evaluation, particularly when the argument of the Bessel functions is large and a large number of terms would be required to sum the series to acceptable accuracy, is

$$P(\theta,\phi) = e^{ikz_o\cos\theta} \frac{e^{i\pi/4}}{\sqrt{\pi}} \left\{ e^{id'\cos(\phi-\phi_o)} F(-\sqrt{2d'}\cos\tfrac{1}{2}(\phi-\phi_o)) \mp e^{id'\cos(\phi+\phi_o)} F(-\sqrt{2d'}\cos\tfrac{1}{2}(\phi+\phi_o)) \right\} \qquad (3)$$

where $d' = k\rho_o \sin\theta$, F(x) is the Fresnel integral

$$F(x) = \int_x^\infty e^{-it^2}\, dt \qquad (4)$$

and the minus sign is taken (Reference 2, Chapter 8).

9. The farfield solution for an acoustically hard baffle is given by the expressions (1) and (2) with the product of the two sine terms replaced by a product of cosine terms, which leads to the representation (3) above with the plus sign.

10. Some useful properties of the Fresnel integral and its numerical evaluation are described in Annex A.

11. Although this model does not represent the true problem of a baffle which is finite in all directions, it is felt that some insight into the dominant features of the physical case may be usefully gained. If attention is restricted to the z=0 plane, i.e. both the source and receiver lie in this plane ($z_o = 0$, $\theta = \pi/2$), the simplified half plane geometry is as indicated in Figure 2. In this investigation the sources will lie in the region $0 \leq \phi_o \leq \pi/2$. Then, in terms of the farfield direction ϕ, $\phi = 0^o$ is in the direction of the infinite baffle, $\phi = 90^o$ is normal to the baffle on the same side as the sources, $\phi = 180^o$ is in the direction of the edge of the baffle on the opposite side to the sources, and $\phi = 360^o$ is in the direction of the infinite baffle on the opposite side to the sources. The region of particular interest with respect to the problem of finiteness of baffles is then $90^o \leq \phi \leq 270^o$.

12. The well-known solutions for a point source at a distance d in front of an infinite (in all directions) plane baffle are,

$$P_s(\phi) = 2\, i \sin(kd \sin\phi) \qquad (5)$$

$$P_h(\phi) = 2 \cos(kd \sin\phi) \qquad (6)$$

for soft and hard baffles respectively ($0 \leq \phi \leq \pi$).

THEORETICAL AND NUMERICAL RESULTS

Source on a hard baffle

13. Consider first the case when the source lies on the baffle ($\phi_o = 0$). For a soft baffle the field reduces trivially to zero, as expected, while the result for a hard baffle is,

$$P(\pi/2, \phi) = 2\, \frac{e^{i\pi/4}}{\sqrt{\pi}}\, e^{ik\rho_o \cos\phi}\, F\left(-\sqrt{2k\rho_o}\, \cos\frac{\phi}{2}\right) \qquad (7)$$

14. In particular, in the direction of the baffle edge ($\phi = \pi$) the field is

$$P(\pi/2, \pi) = e^{-ik\rho_o} \qquad (8)$$

and has unit amplitude, independent of the distance of the source from the baffle edge.

15. The usual approximation when considering arrays on hard finite planar baffles is to multiply the directivity pattern derived for an infinite plane baffle by the factor $\frac{1}{2}(1 + \cos\theta')$ where θ' is the angle made with the normal to the baffle. This has the effect of leaving unchanged the broadside pattern while reducing the pressure by one half (6 dB) at endfire, in agreement with the result (8).

16. Also of interest is the field directly behind the baffle, $\phi = 3\pi/2$. Using the large argument approximation to the Fresnel integral, given in Annex A, gives

$$P(\pi/2, 3\pi/2) \sim \frac{e^{i\pi/4} - i\, e^{-ik\rho_o}}{\sqrt{\pi k\rho_o}} \qquad (9)$$

and hence

$$|P(\pi/2, 3\pi/2)| \sim \frac{1}{\pi\sqrt{2\rho_o/\lambda}} \qquad (10)$$

This result shows that the farfield behind a hard baffle falls off at a rate of 3 dB per doubling of distance of the source from the edge of the baffle. For a source one wavelength from the edge, the front to back ratio is approximately 20 dB.

17. Although a large argument approximation has been used to derive the results (9) and (10), the approximation (10) is in error by less than $\frac{1}{2}$ dB for sources as close as half a wavelength to the edge of the baffle.

18. For a source on a hard baffle, Figure 3 shows the effect of moving the source away from the baffle edge. The theoretical observations described above may clearly be seen. It is also interesting to observe that ripples have been introduced into the directivity patterns in the region $0 \leq \phi \leq \pi$, which would not be present with an infinite baffle. In this case of the semi-infinite baffle the number of ripples appears to be $2\rho_o/\lambda$ and their deviation from the 6 dB level grows towards $\phi = 180^\circ$ to about $\pm$ 1 dB.

19. The region $90^\circ \leq \phi \leq 180^\circ$ has been expanded in Figure 4 which also shows, as dotted lines, the infinite baffle pattern, log 2, and the finite baffle approximation, log $(2 \times \frac{1}{2}(1 + \sin\phi))$. It is clear from this Figure that while the modifying function does lead to a correct endfire level, it can significantly underestimate the field of a single source in other directions, and this error increases as the source moves away from the edge of the baffle. Indeed it is always an underestimate for a source as close as $\lambda/2$ to the baffle edge.

Source near a hard baffle

20. For a source at (ρ_o, ϕ_o), not necessarily lying in the baffle, the far-field is

$$P(\pi/2,\phi) = \frac{e^{i\pi/4}}{\sqrt{\pi}} \left\{ e^{ik\rho_o\cos(\phi-\phi_o)} F(-\sqrt{2k\rho_o}\cos\tfrac{1}{2}(\phi - \phi_o)) + e^{ik\rho_o\cos(\phi+\phi_o)} F(-\sqrt{2k\rho_o}\cos\tfrac{1}{2}(\phi + \phi_o)) \right\} \qquad (11)$$

It is interesting to note that at endfire, in the direction of the edge of the baffle, the field has unit amplitude, independent of the position of the source, i.e.

$$P(\pi/2, \pi) = e^{-ik\rho_o \cos\phi_o} \qquad (12)$$

The result (8) for a source lying on a hard baffle is a special case ($\phi_o = 0$) of this more general result.

21. By varying the position of a single source with respect to the baffle, it appears that the pressure levels behind the baffle and fall-off rate with distance from the baffle edge are very similar to those for a source lying on the baffle, whenever the source is nearer to the baffle than to the edge ($\phi_o \leq \pi/4$). These results are summarised in Table 1. The values given in brackets in the first column are those obtained using the approximate formula (10).

Array on a hard baffle

22. In order to illustrate the behaviour of an array in the presence of a hard finite baffle, a line of nine half wavelength spaced sources with the end element being a half wavelength from the edge of the baffle has been considered. Figure 5 shows the unsteered normalised directivity pattern as a continuous line with the usual infinite baffle pattern superimposed as a dotted line for $0^\circ \leq \phi \leq 180^\circ$. In the region of interest, $90^\circ \leq \phi \leq 180^\circ$, the patterns remain almost identical until very near the endfire direction (180°) with a difference of less than 1 dB in the penultimate sidelobe at about 140°, but a fall of 6 dB at endfire for the finite baffle pattern.

23. Figure 6 shows the pattern for the same array steered in the direction $\phi = 150^\circ$ (i.e. 60° from broadside) with the infinite baffle pattern superimposed. In this case the difference at endfire is 6.5 dB but that fall is relative to 150° where both patterns are normalised. The patterns are very similar from 90° to 150°.

24. Although not shown, the approximate factor of $\frac{1}{2}(1 + \cos\theta')$ discussed previously would modify the unsteered infinite baffle pattern reasonably well giving the correct endfire level. The appropriate reduction in each direction may be seen in Figure 4. However, for the steered pattern it would predict a drop of only $3\frac{1}{2}$ dB between 150° and 180° compared with the actual $6\frac{1}{2}$ dB fall.

25. It is not intended here to carry out a thorough study to determine either one or a set of modifying functions to be applied to infinite baffle directivity patterns to account for finite baffles. However, an improved approximation would appear to be a factor of the form

$$\frac{1}{2}\left(1 + \cos\left(\frac{\theta' - \alpha}{1 - 2\alpha/\pi}\right)\right) \qquad \alpha \leq \theta' \leq \pi/2$$

to be applied within about 30° of endfire i.e. $\alpha = \pi/3$. This factor is a scaled version of the usual factor in order to leave unchanged the pattern from broadside to α and then reduce it smoothly giving a maximum reduction at 6 dB at endfire.

26. A factor of this form is consistent with the patterns of a single point source shown in Figure 4. A suitable value of α will clearly depend on such factors as the number of sources, the steering direction and the baffle size,

although for moderate-sized arrays with baffles extending by up to a half wavelength, a value of $\alpha \sim 60^\circ$, 70° would probably be appropriate. In Figures 7 and 8 the infinite baffle patterns with the modifying factor suggested above (with $\alpha = \pi/3 = 60^\circ$) are superimposed upon the finite baffle patterns for comparison. Good agreement is observed.

27. Figure 9 shows the same array steered to endfire although the resultant main beam is only in the direction 69° from broadside. The modified infinite baffle pattern is shown superimposed (with $\alpha = \pi/3$) and again there is close agreement in the region of the main beam, which is in the direction 72° from broadside. Note that the unmodified infinite baffle pattern has a main beam exactly at endfire. In this case, relative to the main beam level, the finite baffle pattern has sidelobe levels increased by 3-4 dB. If the original modifying function is taken (i.e. $\alpha = 0$) there is better agreement in the region of the sidelobes but the shape of the main beam (now estimated in the direction 74° from broadside) is considerably in error, as shown in Figure 10.

Source near a soft baffle

28. For a source at (ρ_o, ϕ_o) in the presence of a soft half plane, the normalised farfield is given by

$$P(\pi/2,\phi) = \frac{e^{i\pi/4}}{\sqrt{\pi}} \left\{ e^{ik\rho_o\cos(\phi-\phi_o)} F\left(-\sqrt{2k\rho_o}\cos\tfrac{1}{2}(\phi-\phi_o)\right) - e^{ik\rho_o\cos(\phi+\phi_o)} F\left(-\sqrt{2k\rho_o}\cos\tfrac{1}{2}(\phi+\phi_o)\right) \right\} \quad (13)$$

29. At endfire in the direction of the baffle edge ($\phi = \pi$) it may be shown that the farfield is approximately,

$$P(\pi/2,\pi) \sim 2\, e^{i\pi/4}\, e^{-ik\rho_o\cos\phi_o}\, \sqrt{\phi_o\, d_o/\lambda} \quad (14)$$

for source positions such that ϕ_o and d_o/λ are small, where $d_o = \rho_o \sin\phi_o$ is the distance of the source from the baffle. This indicates that the field at endfire for a source near a finite soft baffle falls off at a rate of 3 dB per doubling of distance from the baffle edge (at a constant distance from the baffle), and increases by 6 dB as the distance from the baffle doubles (at a constant distance from the edge).

30. After some analysis it may also be shown that the farfield directly behind the baffle may be approximated as

$$P(\pi/2,\, 3\pi/2) \sim \frac{e^{i\pi/4}}{\sqrt{\pi k\rho_o}}\; i\; e^{-ik\rho_o}\; \frac{\phi_o}{2} \quad (15)$$

for large ρ_o/λ and small ϕ_o. Hence,

$$|P(\pi/2,\, 3\pi/2)| \sim \frac{\phi_o}{2\pi\sqrt{2\rho_o/\lambda}} \sim \frac{\phi_o^{3/2}}{2\pi\sqrt{2d_o/\lambda}} \quad (16)$$

This result shows that the field increases by 6 dB as the distance of the source from the baffle doubles (at constant distance from the edge), and decreases by by 9 dB as the distance from the baffle edge doubles (for constant distance d_o from the baffle).

31. These results have been verified by computing the farfield pressure using the exact expression (13). The full directivity patterns for a source at $\frac{1}{4}$ wavelength from the baffle and various distances from the baffle edge are shown in Figure 11. A summary of the results obtained by varying the position of a single source near a soft baffle is given in Tables 2 and 3. The approximations (14) and (16) are given in brackets whenever they are within about 3 dB of the true values, clearly demonstrating the validity of these approximations.

Array near a soft baffle

32. The same nine-element point source array previously described is now considered at a distance of one quarter wavelength from a soft half plane. The unsteered directivity pattern is shown in Figure 12 with the infinite soft baffle pattern superimposed as a dotted line. The two patterns are almost identical until very near endfire where the infinite baffle pattern predicts a null while the effect of the finite baffle is to allow sound to diffract behind the baffle.

33. Figure 13 shows the same array steered 60° from broadside, although for both the finite and infinite baffle patterns the main beam is actually only steered to 57°. Similarly Figure 14 shows the effect of steering to endfire with both the resultant beams being only 68° from broadside.

34. In each of these examples the only significant effect of the finite baffle is to give a non-zero field in the endfire direction and behind the baffle. In front of the baffle the sidelobe levels and directions change very little from the more easily computed infinite baffle pattern, and as a first approximation it does not appear necessary to modify the infinite baffle pattern to account for a finite soft baffle.

DISCUSSION AND CONCLUSIONS

35. The preceding results have been derived for the ideal case of perfectly thin hard or soft baffles with no transmission through the baffle. In practice in water soft baffles can be made relatively thin whilst an effective thin hard baffle is difficult to achieve. In air the reverse is true. The consideration of baffles with finite thickness and also finite impedance is a considerably more complex problem for which some rigorous and approximate analyses are possible. (References 3 and 4).

36. Also, only the farfield of a source in the presence of a half plane has been considered. The nearfield may be calculated if required, an eigenfunction series solution having been given for the general case of a wedge of arbitrary angle in Reference 1 (equation (2)).

37. Under these restrictions, and when a source is close to one edge of a baffle only, some useful approximations are valid for sources "near" the baffle.

a. Hard baffle: The field of a point source at endfire is 6 dB lower than the maximum broadside value, and directly behind the baffle it falls off at a rate of 3 dB per doubling of distance of the source from the edge of the baffle. These results are independent of the shortest distance of the source from the baffle.

b. Soft baffle: The field of a point source at endfire falls off at a rate of 3 dB per doubling of distance from the edge of the baffle, while the field directly behind the baffle falls off at a rate of 9 dB per doubling of distance. In each case as the shortest distance of the source from the baffle doubles, the pressure rises by 6 dB.

c. Arrays: The effect of a finite baffle on the directivity pattern of an array is significant mainly near endfire, particularly if an attempt is made to steer the beam in this direction. For a hard baffle it is necessary to modify the infinite baffle pattern and an appropriate factor has been discussed. For a soft finite baffle there is closer agreement with the infinite baffle pattern where the inability to steer towards endfire is already apparent, and no modifying factor has been suggested.

REFERENCES

Reference

1 D. T. Wilton, "The pressure field of hydrophones in the presence of a wedge-shaped baffle", A.U.W.E. Div Note (1978).

2 J. J. Bowman, T. B. A. Senior and P. L. E. Uslenghi, "Electromagnetic and Acoustic Scattering by Simple Shapes*, 1969, North-Holland Publishing Company - Amsterdam.

3 A. D. Pierce, "Diffraction of sound around corners and over wide barriers", (1974), J.A.S.A. 55, 941-955.

4 A. D. Pierce and W. J. Hadden Jr., "Plane wave diffraction by a wedge with finite impedance", (1978), J.A.S.A. 63, 17-27.

5 Collected Algorithms from CACM, ACM New York.

ANNEX A - THE FRESNEL INTEGRAL

1. The complex Fresnel integral

$$F(x) = \int_x^\infty e^{-it^2}\,dt \tag{A1}$$

may be expressed in real and imaginary parts as,

$$F(x) = \sqrt{\frac{\pi}{2}}\left\{\left[\frac{1}{2} - C\left(\sqrt{\frac{2}{\pi}}\,x\right)\right] - i\left[\frac{1}{2} - S\left(\sqrt{\frac{2}{\pi}}\,x\right)\right]\right\} \tag{A2}$$

where

$$C(u) = \int_0^u \cos\left(\frac{\pi}{2}\,t^2\right)dt \tag{A3}$$

and

$$S(u) = \int_0^u \sin\left(\frac{\pi}{2}\,t^2\right)dt \tag{A4}$$

are the Fresnel cosine and sine integrals respectively.

Now,

$$F(x) + F(-x) = 2F(0) \tag{A5}$$

and $$F(0) = \frac{1}{2}\sqrt{\frac{\pi}{2}}\,(1 - i) \tag{A6}$$

For small x,

$$C(x) \sim x \tag{A7}$$

and $$S(x) \sim \frac{\pi x^3}{6} \tag{A8}$$

For large x,

$$F(x) \sim \frac{i}{2x}\,e^{-ix^2} \qquad x \to +\infty \tag{A9}$$

2. The numerical results presented in this note have been based upon the numerical evaluation of Fresnel cosine and sine integrals given by CACM Algorithm 244 (Reference 5) where further details of the particular small and large argument series employed may be found.

Distance from baffle edge ($\rho_o \cos \phi_o$) \ Distance from baffle ($\rho_o \sin \phi_o$)	0	$\lambda/2$	λ	2λ	4λ
0	0	- 4.6	- 5.0	- 5.3	- 5.5
$\lambda/2$	-10.3 (-9.9)	-10.0	- 9.5	- 8.8	- 8.2
λ	-13.1 (-13.0)	-12.9	-12.5	-11.7	-10.6
2λ	-16.0 (-16.0)	-15.9	-15.8	-15.3	-14.2
4λ	-19.0 (-19.0)	-19.0	-18.9	-18.7	-18.2

Table 1 Pressure levels (dB) in the farfield directly behind ($\phi = 3\pi/2$) a hard half plane baffle due to a point source.

Distance from baffle edge ($\rho_o \cos \phi_o$)	Distance from baffle ($d_o = \rho_o \sin \phi_o$)				
	$\lambda/4$	$\lambda/2$	λ	2λ	4λ
0	2.0 (2.0)	2.0	-1.5	-1.0	-0.7
$\lambda/2$	-3.3 (-3.3)	1.5 (2.0)	0.7	0.7	0.6
λ	-6.1 (-6.1)	-0.5 (-0.3)	2.5 (5.0)	1.1	0.0
2λ	-9.1 (-9.1)	-3.1 (-3.1)	1.9 (2.7)	-2.2	1.0
4λ	-12.0 (-12.0)	-6.1 (-6.0)	-0.3 (-0.1)	2.2 (5.7)	-0.1

Table 2 Pressure levels (dB) in the farfield at endfire ($\phi = \pi$) of a soft half plane baffle due to a point source.

Distance from baffle ($d_o = \rho_o \sin \phi_o$)

Distance from baffle edge ($\rho_o \cos \phi_o$)	$\lambda/4$	$\lambda/2$	λ	2λ	4λ
0	-8.2 (-9.0)	-7.5	-7.0	-6.7	-6.5
$\lambda/2$	-23.6 (-23.1)	-18.5 (-19.6)	-14.5	-11.8	-9.9
λ	-31.6 (-31.3)	-25.8 (-26.1)	-20.5 (-22.6)	-16.3	-13.1
2λ	-40.2 (-40.1)	-34.2 (-34.3)	-28.4 (-29.1)	-23.0 (-25.6)	-18.5
4λ	-49.1 (-49.1)	-43.1 (-43.1)	-37.1 (-37.3)	-31.3 (-32.2)	-25.9 (-28.6)

Table 3 Pressure levels (dB) in the farfield directly behind ($\phi = 3\pi/2$) a soft half plane due to a point source.

FIG. 1.

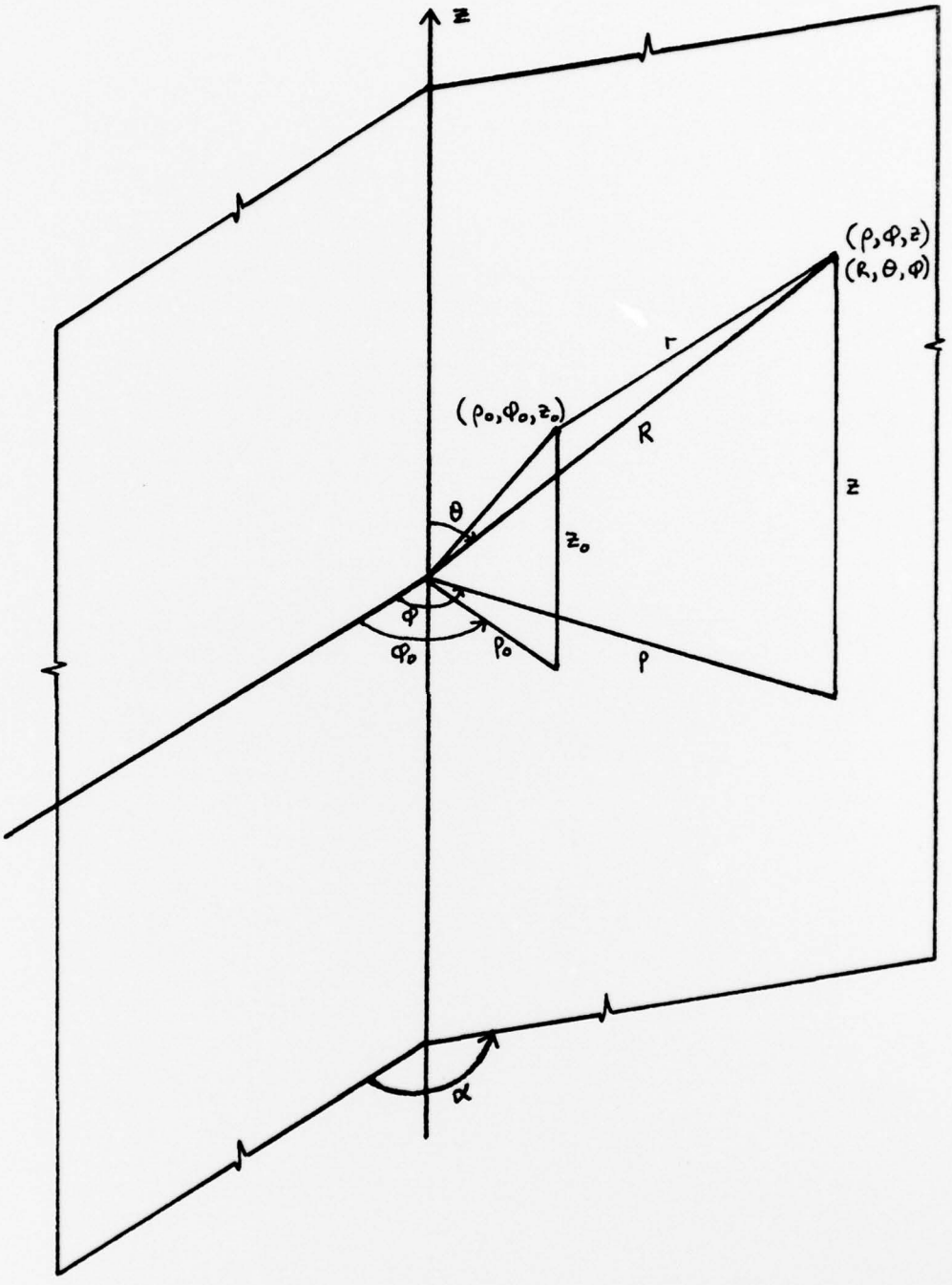

Figure 1 Wedge geometry

FIG. 2.

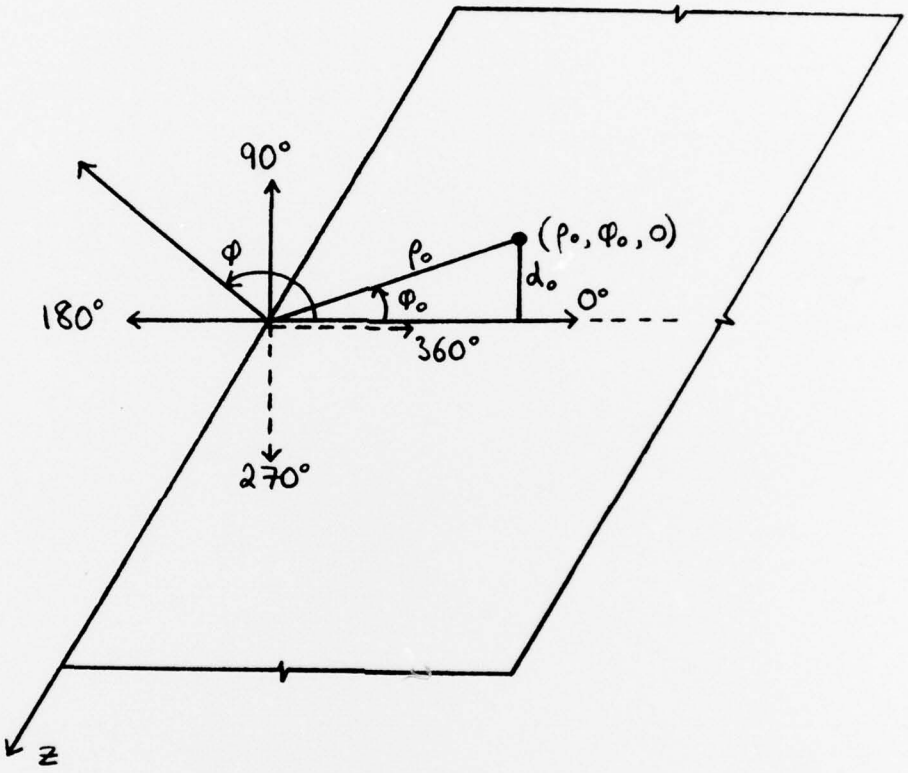

Figure 2 Half plane geometry

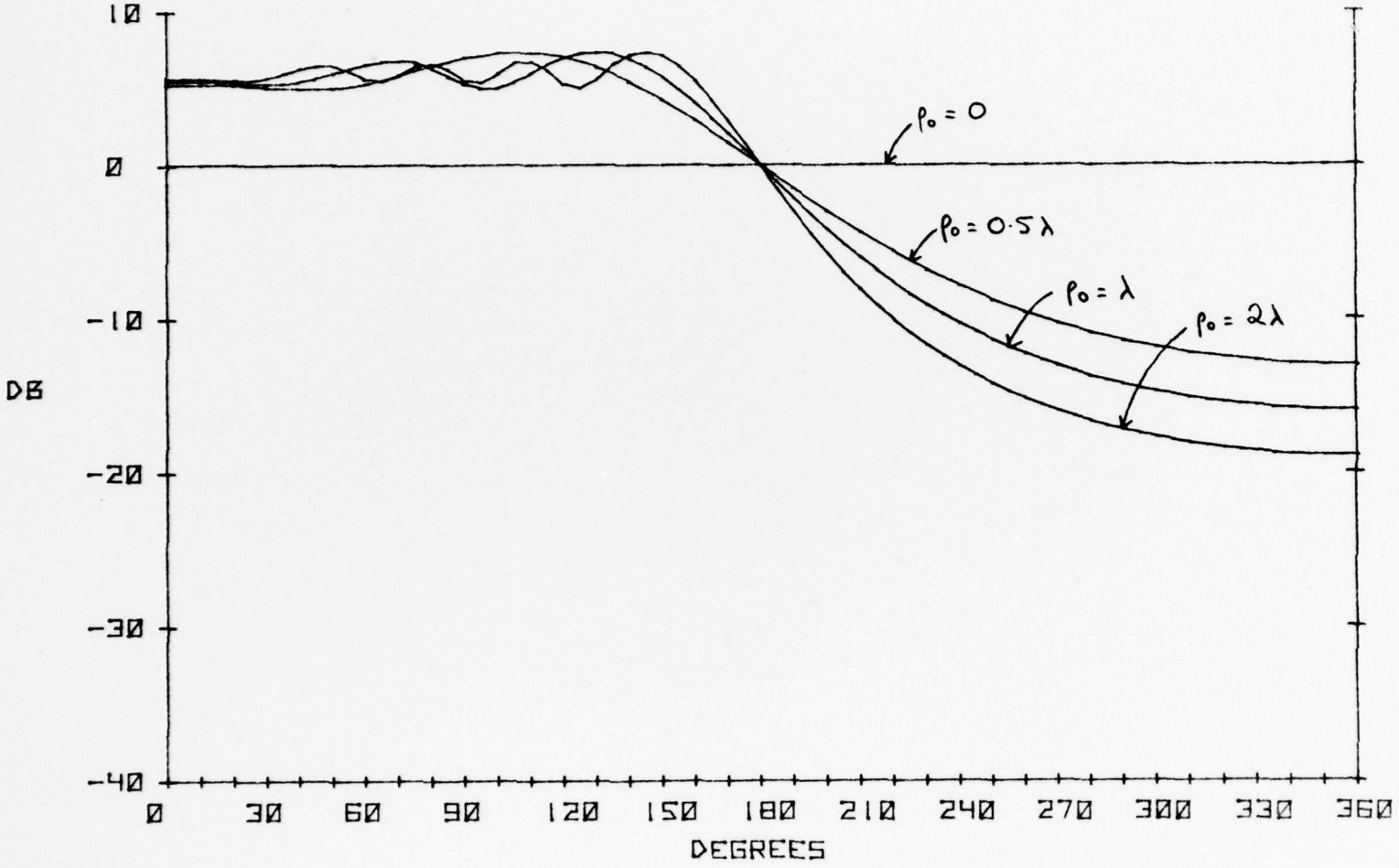

Figure 3 Directivity patterns of single sources on a hard half plane

FIG. 3.

FIG. 4

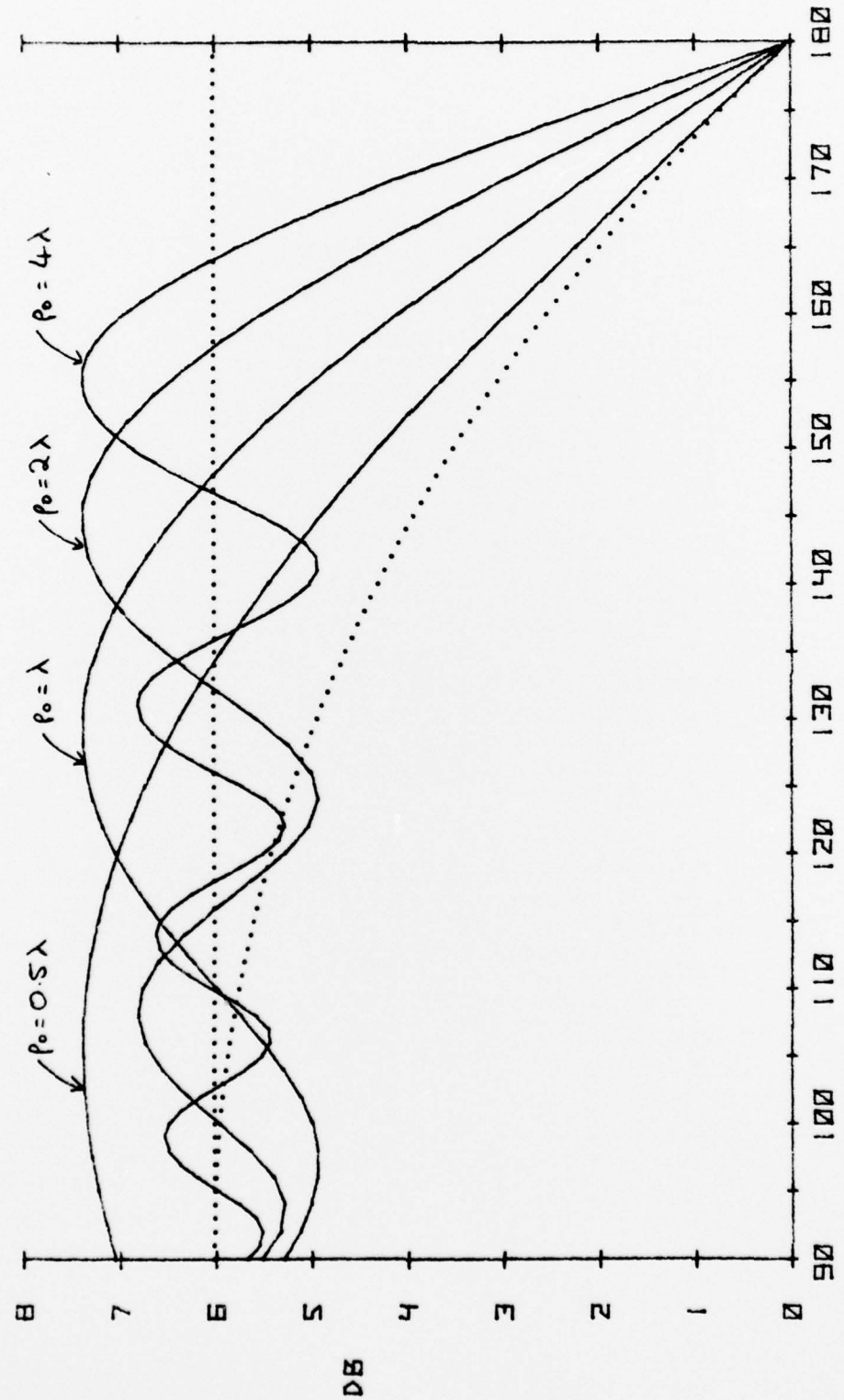

Figure 4 Directivity patterns of single sources on a hard half plane

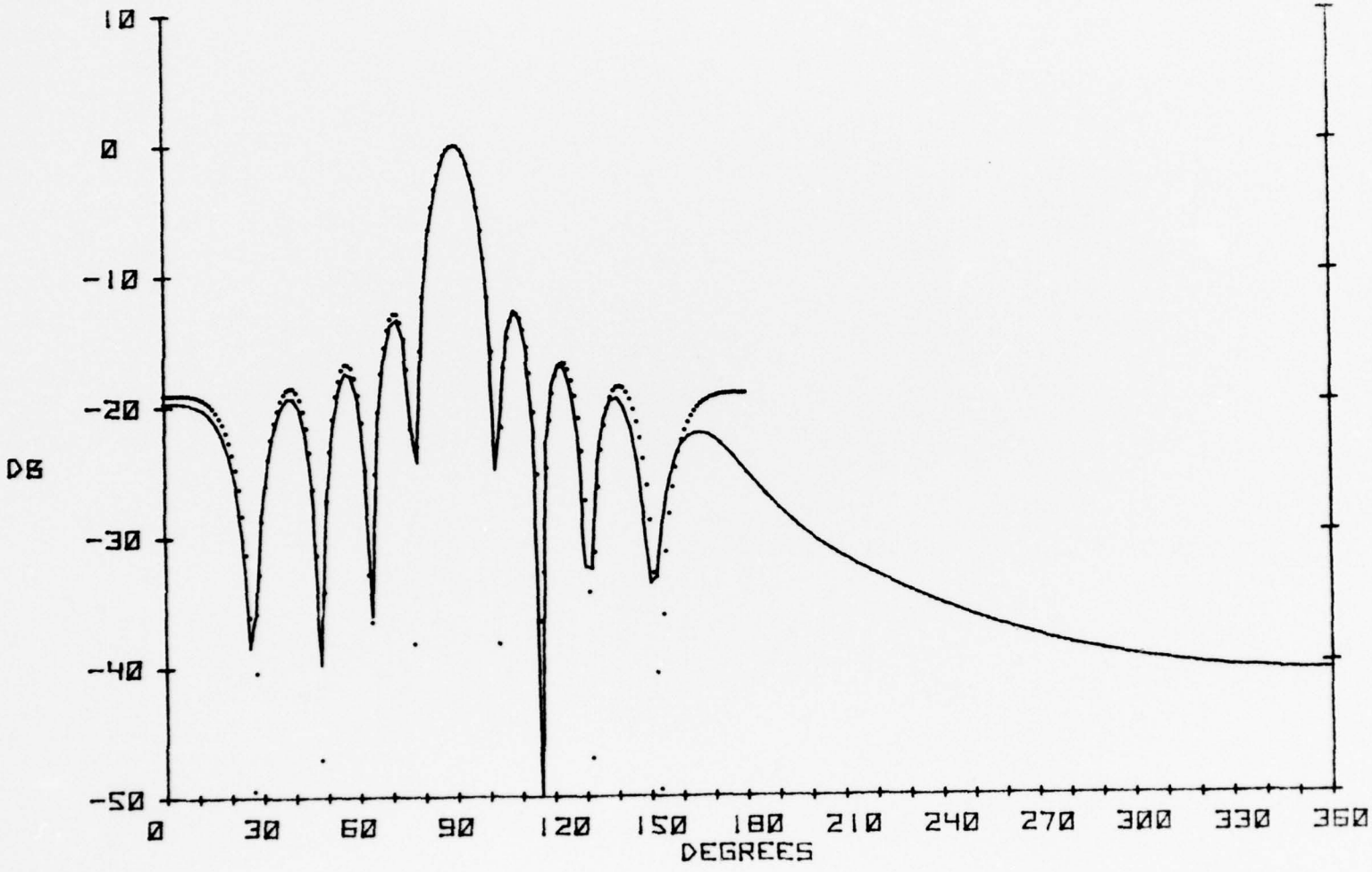

Figure 5 Directivity pattern of an unsteered nine-element line array on a hard half plane

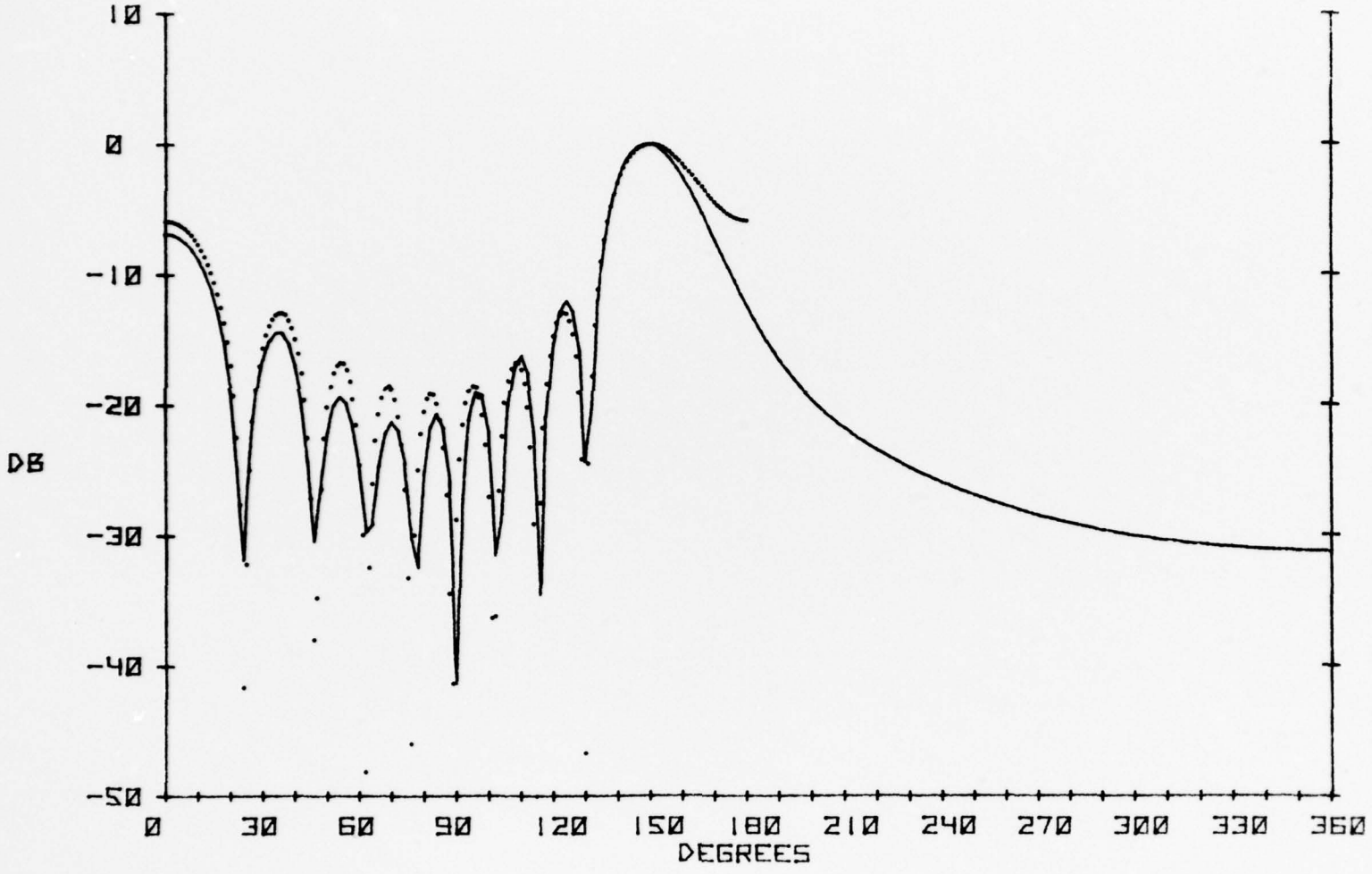

Figure 6 Directivity pattern of a nine-element line array on a hard half plane, steered 60° from broadside

FIG. 6

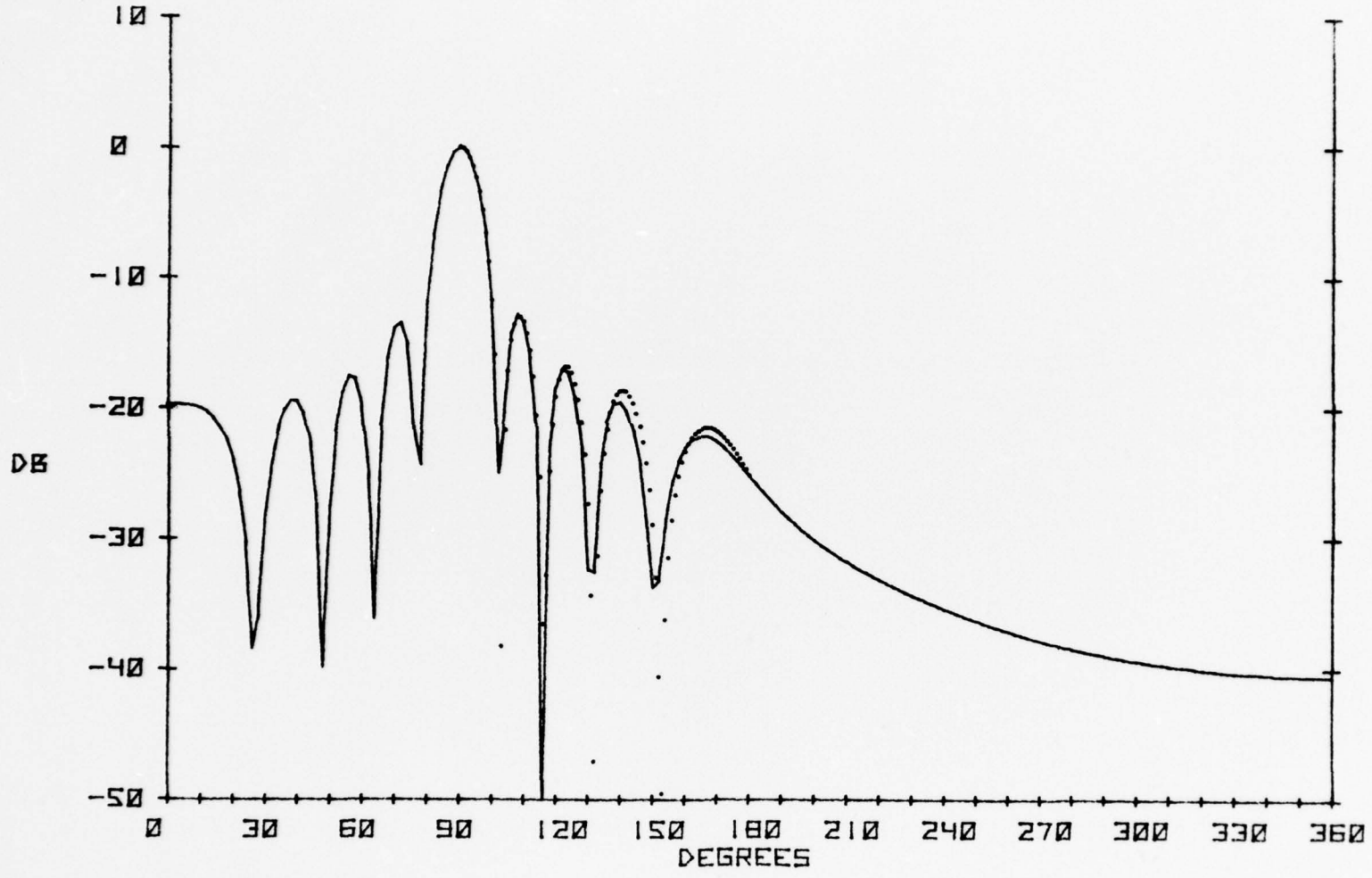

Figure 7 Directivity pattern of an unsteered nine-element line array on a hard half plane

FIG. 7.

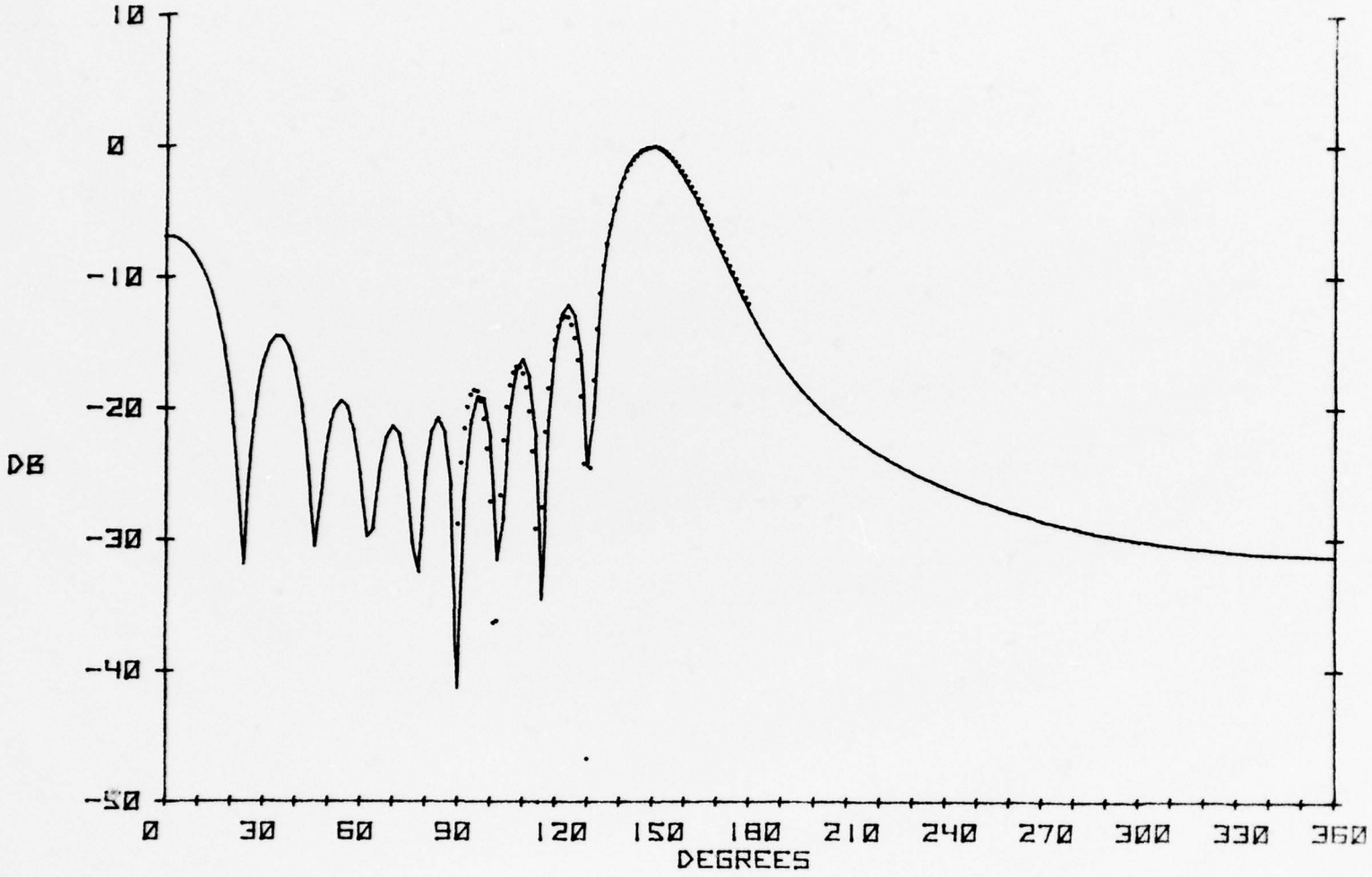

Figure 8 Directivity pattern of a nine-element line array on a hard half plane, steered 60° from broadside

FIG. 8

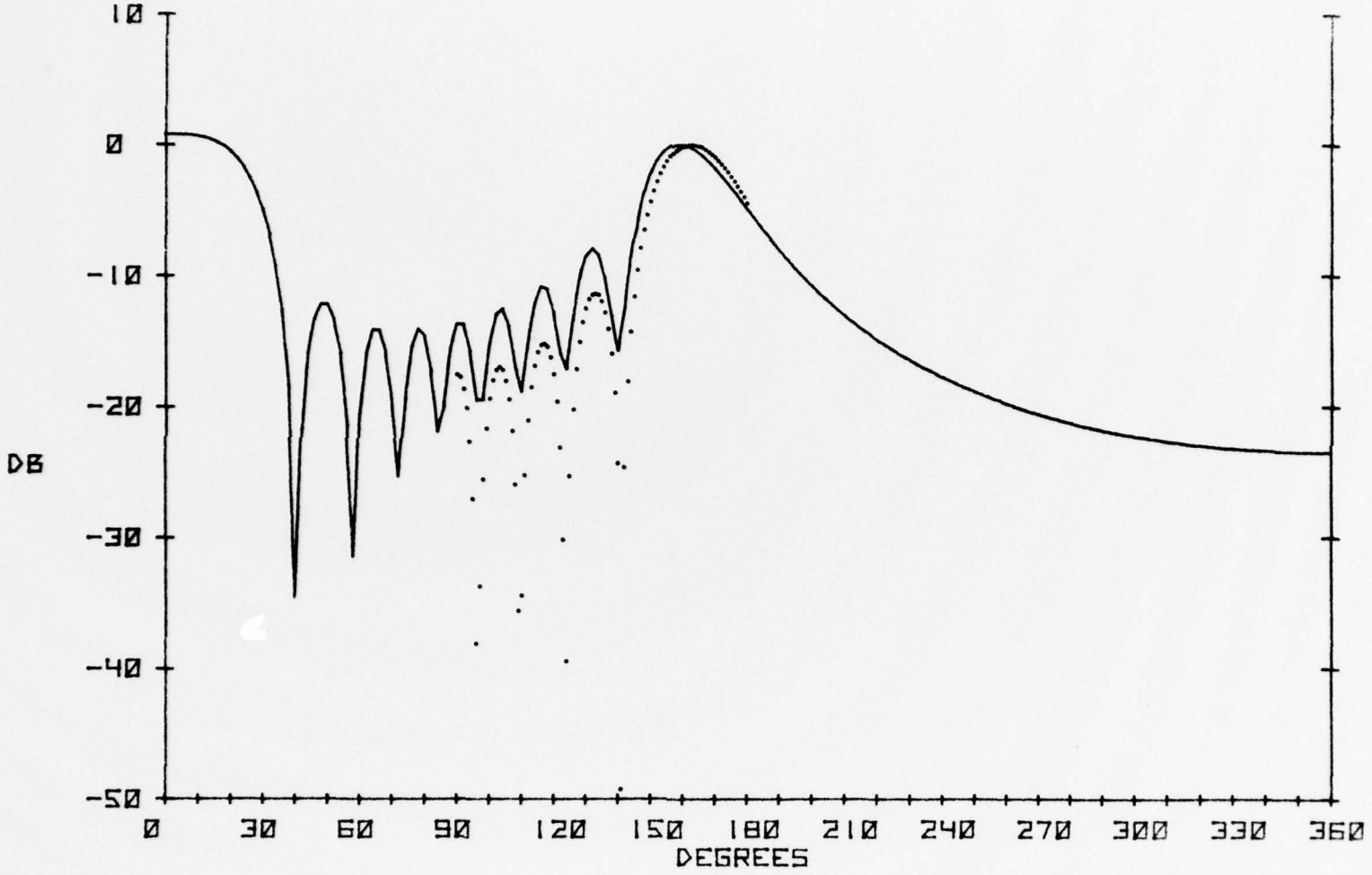

Figure 9 Directivity pattern of a nine-element line array on a hard half plane steered to endfire

FIG. 9.

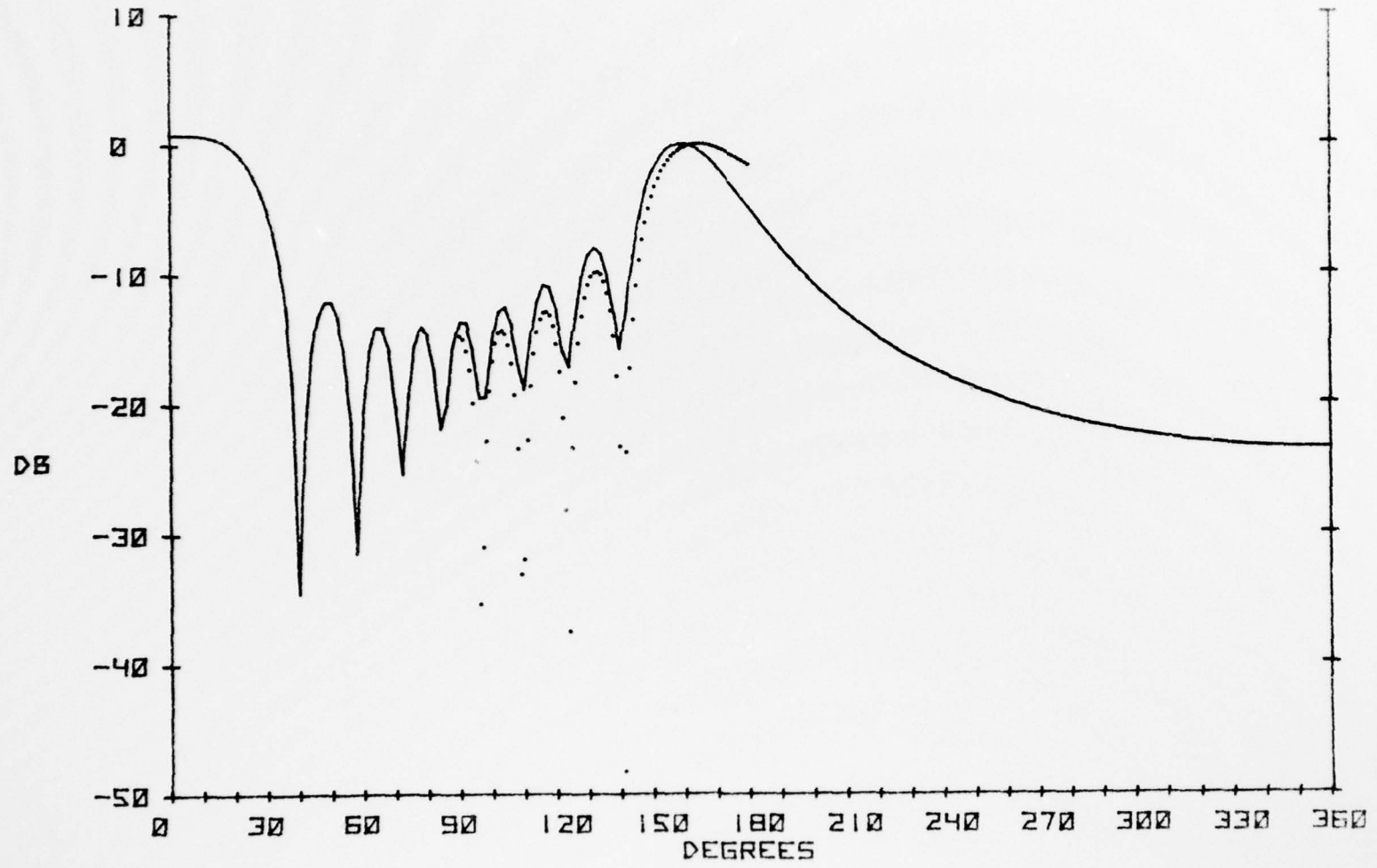

Figure 10 Directivity pattern of a nine-element line array on a hard half plane steered to endfire

FIG. 10

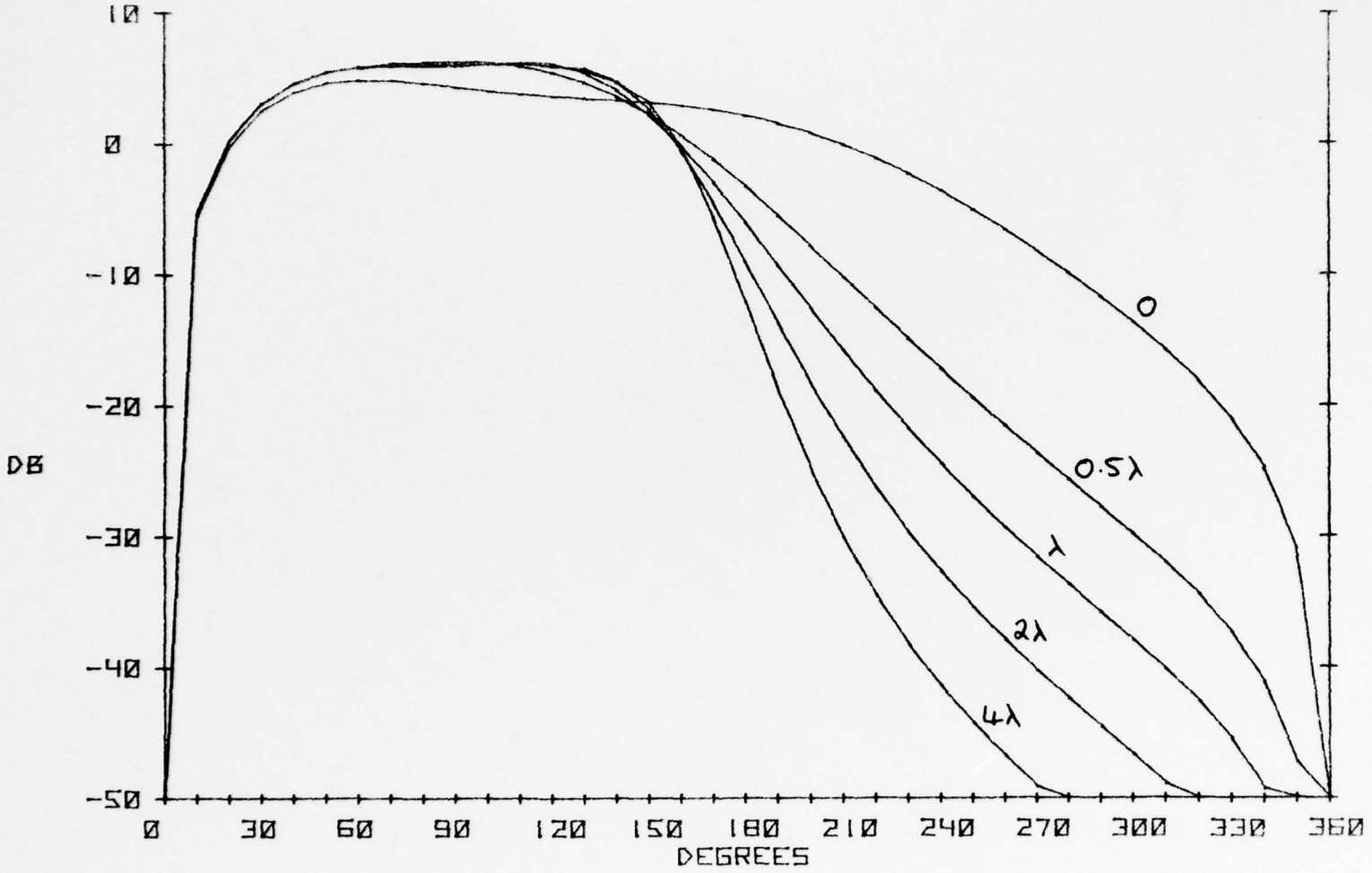

Figure 11 Directivity patterns of single sources at one quarter wavelength from a soft half plane

FIG. 11.

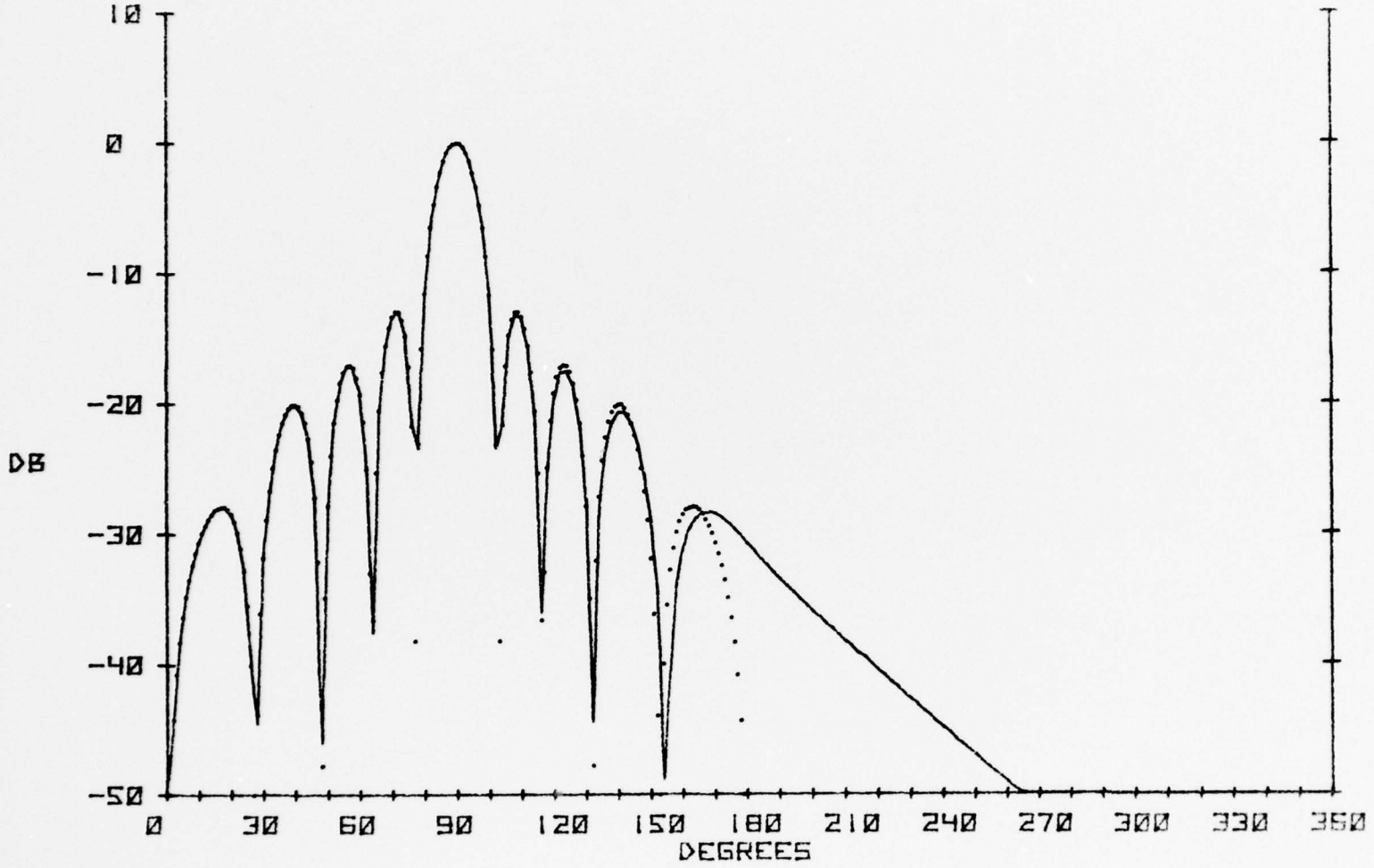

Figure 12 Directivity pattern of an unsteered nine-element line array near a soft half plane

FIG. 12

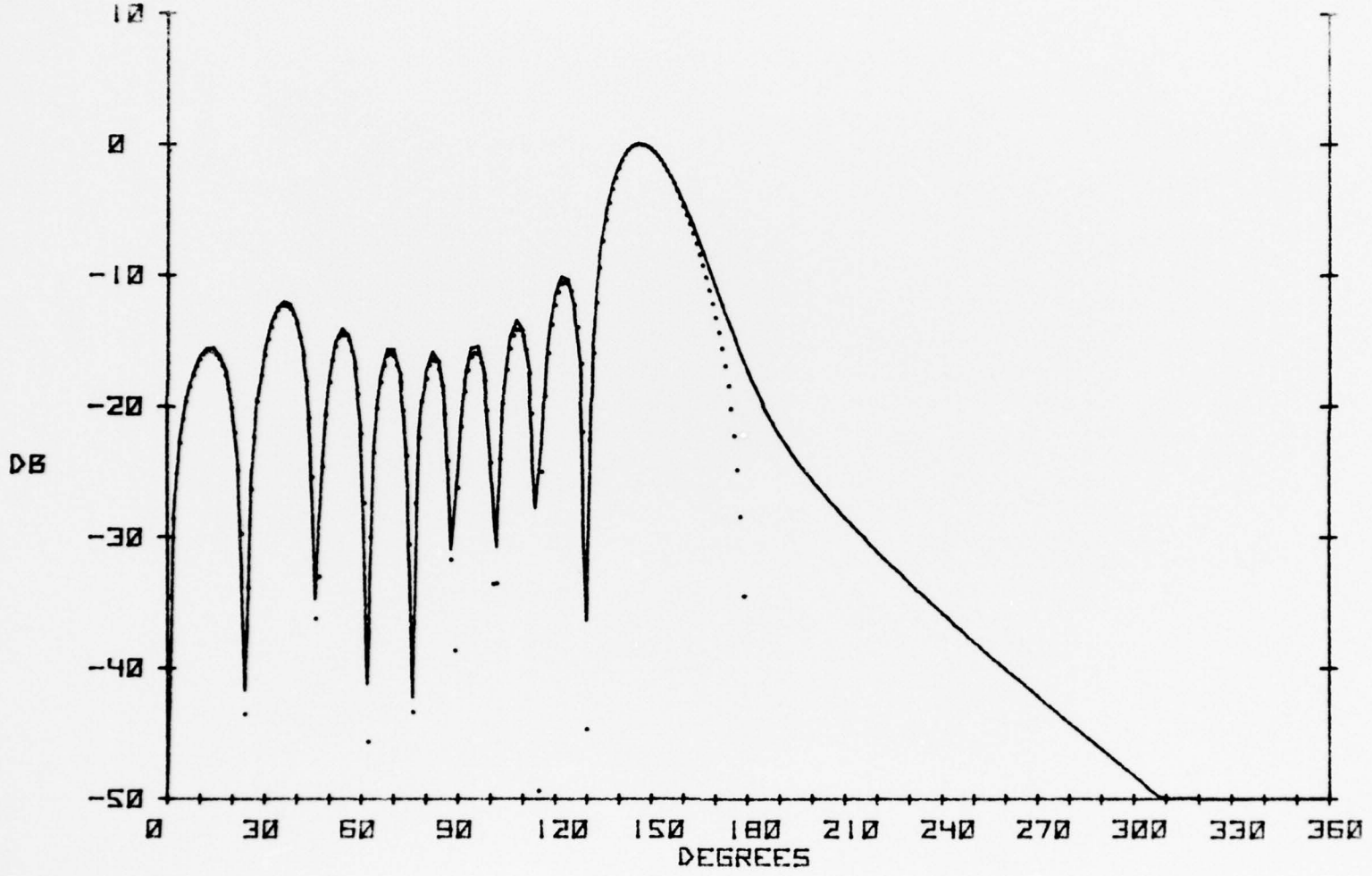

Figure 13 Directivity pattern of a nine-element line array near a soft half plane, steered 60° from broadside

FIG. 13

FIG.14

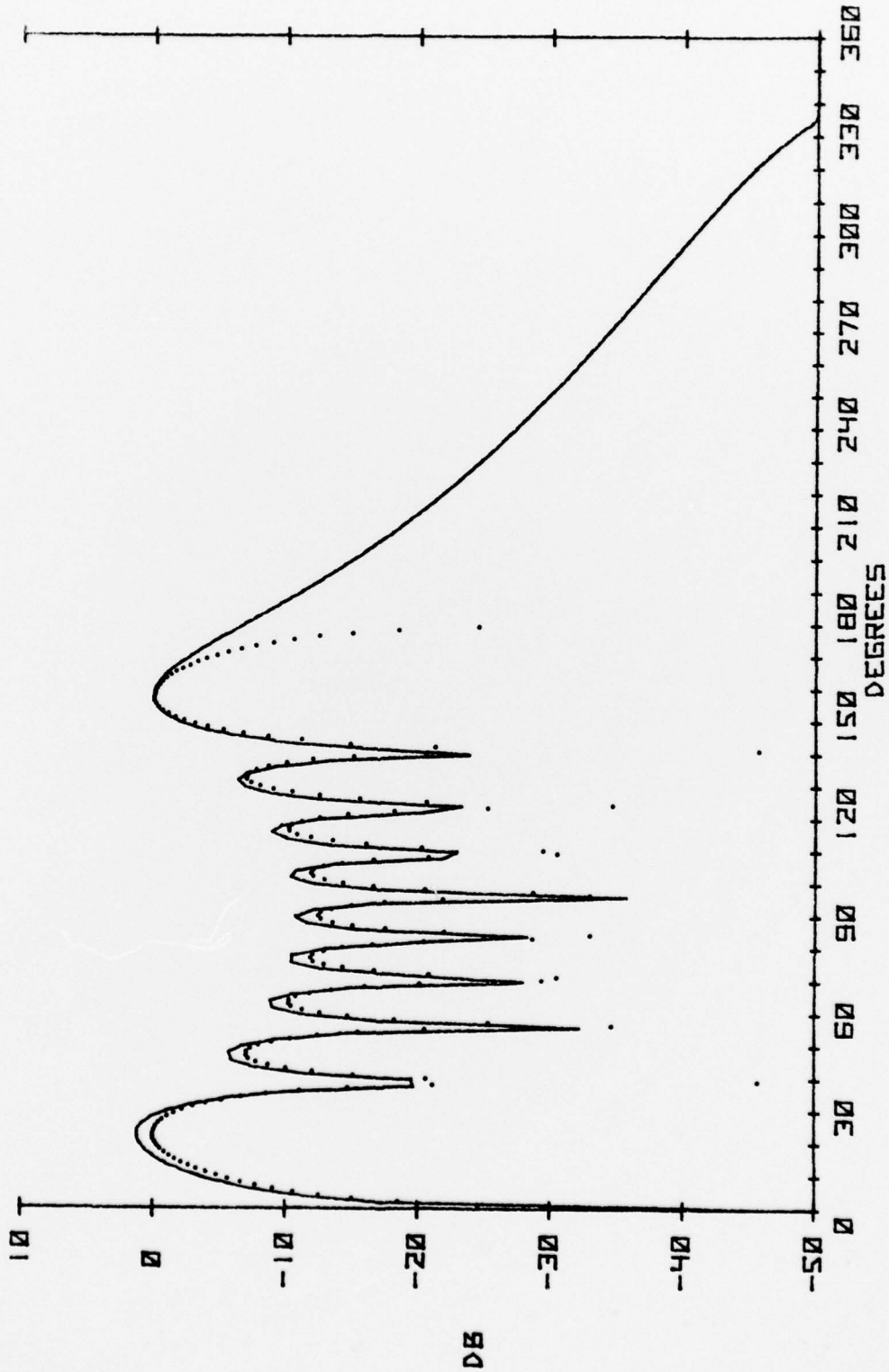

Figure 14 Directivity pattern of a nine-element line array near a soft half plane, steered to endfire